Science of the Total Environment 859 (2023) 160104

Contents lists available at ScienceDirect

Science of the Total Environment

journal homepage: www.elsevier.com/locate/scitotenv

Mixed bromine/chlorine transformation products of tetrabromobisphenol A formed in the combustion of printed circuit boards: Emission characteristics and transformation pathways

Xiang Ge, Yanpeng Gao, Yan Yang *, Guanhui Chen, Shengtao Ma, Beibei Hu, Yingxin Yu, Taicheng An

Guangdong-Hong Kong-Macao Joint Laboratory for Contaminants Exposure and Health, Guangdong Key Laboratory of Environmental Catalysis and Health Risk Control, Institute of Environmental Health and Pollution Control, Guangdong University of Technology, Guangzhou 510006, PR China

Guangzhou Key Laboratory of Environmental Catalysis and Pollution Control, Key Laboratory of City Cluster Environmental Safety and Green Development, School of Environmental Science and Engineering, Guangdong University of Technology, Guangzhou 510006, PR China

HIGHLIGHTS

- The emission factor of Br_xBPAs was highest during the printed circuit board combustion.
- Cl_yBr_xBPA formation was limited because of less chlorine in printed circuit boards.
- Most combustion products were partitioned into the oil and particle phases.
- The emission rates of TBBPA and its transformation products peaked at 300 °C.
- Radical substitution reaction "–•Br + •Cl" of Br_xBPAs governed Cl_yBr_xBPA formation.

GRAPHICAL ABSTRACT

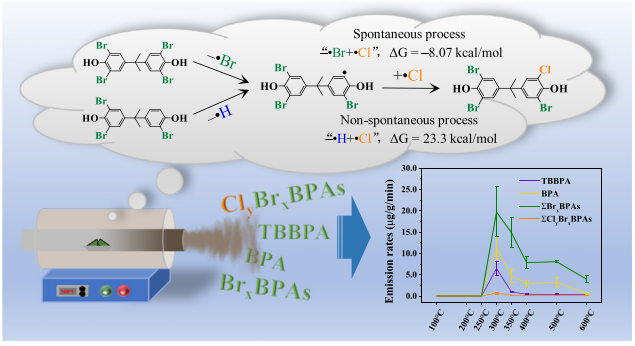

ARTICLE INFO

Editor: Shuzhen Zhang

Keywords:
Emission factor
Mixed halogenated compound
Quantum chemical calculation
Transformation pathway
Radical substitution reaction

ABSTRACT

Recently, mixed bromine/chlorine transformation products of tetrabromobisphenol A (Cl_yBr_xBPAs) were found to be possibly related to the thermal treatment processes of electronic wastes. To explore their emission characteristics and formation mechanism, printed circuit board scraps were combusted in a tube furnace, under the temperature from 25 °C to 600 °C. The emission factor of the debromination products of tetrabromobisphenol A (Br_xBPAs) was the highest, whereas that of Cl_yBr_xBPAs was the lowest. Among three phases, most of the target compounds were partitioned into the oil and particle phases, and only negligible gaseous 2-BrBPA and bisphenol A were detected. The emission rates of most compounds were fastest at 300 °C, although 2-BrBPA, 2,6-Br_2BPA, and 2-Cl-6-BrBPA peaked at 350 °C. Among the chemicals in total emission, 2-BrBPA was the dominant congener in Br_xBPAs, whereas 2-Cl-2′,6,6′-Br_3BPA, 2-Cl-2′,$6^{\#}$-Br_2BPA, and $\Sigma_2Cl_1Br_1BPAs$ shared similar proportions in Cl_yBr_xBPAs. Meanwhile, the composition profiles at 300 °C showed that 2,2′,6-Br_3BPA and 2-Cl-2′,6,6′-Br_3BPA occupied the largest proportions in Br_xBPAs and Cl_yBr_xBPAs, respectively. To reveal the possible transformation pathways, the Gibbs free energy was calculated based on a radical substitution reaction. After "•Br" removal from bisphenol A or other Br_xBPAs, the intermediate was more easily combined with "•H" than with "•Cl." In addition, the Cl_yBr_xBPA formation via "–•H + •Cl" by Br_xBPAs is nonspontaneous, thus limiting the further generation of Cl_yBr_xBPAs. This study not only provides ideas for the study of other mixed halogenated products, but also provides constructive suggestions for environmental source analysis by combining previous research on the occurrence of Cl_yBr_xBPAs in various environmental matrices.

* Corresponding author at: Guangdong-Hong Kong-Macao Joint Laboratory for Contaminants Exposure and Health, Guangdong Key Laboratory of Environmental Catalysis and Health Risk Control, Institute of Environmental Health and Pollution Control, Guangdong University of Technology, Guangzhou 510006, PR China.
E-mail address: yangyan1209@gdut.edu.cn (Y. Yang).

http://dx.doi.org/10.1016/j.scitotenv.2022.160104
Received 17 October 2022; Received in revised form 6 November 2022; Accepted 6 November 2022
Available online 11 November 2022

1. Introduction

Tetrabromobisphenol A (TBBPA), as a polybrominated flame retardant, is often added to materials to enhance fire safety (Liu et al., 2016). Typically, brominated epoxy resins, which are synthesized from bisphenol A (BPA, doped with TBBPA) and epichlorohydrin, are commonly coated on fiberglass for the manufacture of FR-4 printed circuit boards (Hall and Williams, 2007; Krol et al., 2003). However, excessive addition leads to some unreacted TBBPA (0.02 wt%) remaining in the resins in molecular form (Zhou et al., 2014). This unreacted TBBPA can be released into the environment during the usage and the final recycling processes of the resin products. To date, TBBPA has been found in various environmental matrices, such as water, sediment, soil, dust, air, and biota, and the pollution levels in electronic waste (e-waste) dismantling areas are obviously higher than in other areas (Feng et al., 2012; Huang et al., 2014; Ni and Zeng, 2013; Sjodin et al., 2001; Xu et al., 2013; Yang et al., 2012; Zhou et al., 2014).

For the modern e-waste recycling industry, high temperature is an indispensable condition, wherein printed circuit boards are baked to peel off electronic components, and nonferrous and precious metals are recovered by pyrometallurgy (Kaya, 2016). Driven by heat, the flame retardants in resins are inevitably released accompanied by transformation. Many studies have simulated open burning and tube furnace experiments of e-waste and reported the emission characteristics of flame retardants and their transformation products (Cai et al., 2019; Chiang and Lin, 2014; Duan et al., 2011; Li et al., 2018, 2019a, 2019b). Among them, various flame retardants, volatile organic compounds, polycyclic aromatic hydrocarbons, and halogenated dioxins and furans have attracted the most concern (Cai et al., 2019; Chiang and Lin, 2014; Duan et al., 2011; Li et al., 2018, 2019a, 2019b), whereas limited studies focused on mixed halogenated transformation products, such as the formation of mixed halogenated dibenzo-p-dioxins and furans, as well as mixed halogenated diphenyl ethers at elevated temperature in the presence of a chlorine source (Bendig et al., 2012; Roszko et al., 2015; Rupp and Metzger, 2005; Soderstrom and Marklund, 2022). For TBBPA, although its debromination products (Br_xBPAs) have been well researched (Barontini et al., 2004, 2005; Grause et al., 2008; Luda et al., 2002), mixed bromine/chlorine transformation products (Cl_yBr_xBPAs) are not well understood because of the lack of standards. A study reported that the *co*-pyrolysis products of brominated flame retardants and polyvinyl chloride contained Cl_yBr_xBPAs, and initially proposed that their production was dominated by free radical reaction, although no quantitative analysis was conducted (Czegeny et al., 2012). Recently, our group found and identified seven Cl_yBr_xBPAs in the dust of e-waste dismantling areas (Liu et al., 2020), and also detected them in sediment and soil (Chen et al., 2021; Ge et al., 2022). In addition, studies have shown that the toxicities of mixed halogenated transformation products may be equal to or even exceed their parent compounds (Fernandes et al., 2014; Mason et al., 1987; Weber and Greim, 1997). Therefore, more studies should be conducted on these mixed halogenated products.

From the viewpoint of thermodynamics of reactions, the thermodynamic parameters such as the Gibbs free energy change (ΔG) can indicate the favorable of the investigated reaction. Theoretical calculations can obtain readily these thermodynamic parameters and have been developed as an auxiliary method of experiments in labs to explore successfully the reaction mechanism. For instance, the thermodynamic properties of persistent halogenated organic compounds in dehalogenation processes were summarized at different theoretical levels, including semiempirical, ab initio, density functional theory (DFT), and periodic DFT (Luo et al., 2015). In addition, the thermodynamic properties of several polybrominated flame retardants were accurately predicted using a DFT method (Grabda et al., 2007). This showed that the thermodynamic stability of the congeners decreases with the number of Br atoms, and is also related to the substitution position on benzene ring. As for TBBPA, although molecular properties and degradation characteristics based on theoretical calculations have been studied (Huang et al., 2021; Qiu et al., 2013; Wang et al., 2019), there was no information on these for Cl_yBr_xBPAs.

Thus, the present study hypothesized that a tube furnace experiment combined with quantum chemical calculations of reaction energy could deepen the understanding of the emission characteristics and the formation mechanism of Cl_yBr_xBPAs during the e-waste thermal treatment processes. Therefore, this study mainly focused on: (1) the emission factors of TBBPA, Br_xBPAs, BPA, and Cl_yBr_xBPAs, and the partitioning among the oil, particle, and gas phases; (2) the emission rates of the target chemicals and the influence of degradation temperature on the emission; (3) the possible pathways and mechanisms of the transformation products using a theoretical calculation based on ΔG. The results not only described the emission characteristics and transformation pathways of TBBPA and its transformation products well, but found the pollutants' compositional differences between the direct emission and environmental occurrence, providing constructive guidance for the source analysis of environmental monitoring works.

2. Materials and methods

2.1. Chemicals and reagents

TBBPA and BPA were purchased from AccuStandard (New Haven, CT, USA), and the isotope-labeled compounds $^{13}C_{12}$-TBBPA and $^{13}C_{12}$-BPA were purchased from Wellington Laboratories (Guelph, ON, Canada) and Cato Research Chemicals (Eugene, OR, USA), respectively. Transformation products, including four Br_xBPAs (2,2′,6-Br_3BPA, 2,2′-Br_2BPA, 2,6-Br_2BPA, and 2-BrBPA) and seven Cl_yBr_xBPAs (2,2′-Cl_2-6,6′-Br_2BPA, 2,2′-Cl_2-6-BrBPA, 2-Cl-2′,6,6′-Br_3BPA, 2-Cl-2′,6-Br_2BPA, 2-Cl-2′,6′-Br_2BPA, 2-Cl-2′-BrBPA, and 2-Cl-6-BrBPA) were synthesized in our lab and were reported previously (Liu et al., 2020). Acetone, *n*-hexane, acetonitrile, methanol, and acetic acid of high-performance liquid chromatography grade were all obtained from CNW Technologies (Dusseldorf, Germany). The quartz membranes for particle collection were baked at 460 °C for 12 h, and polyurethane foam plugs for the gas product collection were successively Soxhlet extracted using methanol for 24 h and then dichloromethane for 24 h. The bare FR-4 printed circuit boards without copper covering and soldering of electronic components were customized by JLC Co., Ltd. (Shenzhen, China).

2.2. Thermogravimetric analysis and tube furnace experiment

The thermogravimetric characteristics of printed circuit boards were determined using a thermogravimetric analyzer (TGA 2, Mettler-Toledo, Switzerland). Heating rates of 10 °C/min was set and dry air was provided as the reactive gas at a flow rate of 20 mL/min. The temperature range was from 25 to 900 °C.

According to the thermogravimetric analysis, the endpoint of the combustion temperature was set at 600 °C. The combustion device, including a tube furnace (GSL-1100X, Kejing Material Technology Co., Ltd., China) and a product collection system, is shown in Fig. S1. To obtain the emission factors, approximately 0.5 g of printed circuit board scraps were combusted and the products were collected throughout the experiment (25–600 °C). To discuss the emission rates and transformation of the chemicals at different temperatures, approximately 1.0 g of printed circuit board scraps were combusted. Sampling at 100, 200, 250, 300, 350, 400, 500, and 600 °C was performed, and a 3 min constant temperature interval was set for sample collection. A heating rate of 10 °C/min was used and dry air was passively ventilated at a flow rate of 250 mL/min. Each experiment was conducted in triplicate.

2.3. Analytical protocols

The combustion products were sequentially separated through a quartz membrane and a polyurethane foam plug, to obtain particle phase and gas phase, respectively (Fig. S1). Each sample was cut into scraps and wrapped in filter paper, then Soxhlet extracted with a 100 mL mixture of acetone and *n*-hexane (1:1, v/v) for 12 h. For comparison, resin powder on printed

circuit board was also Soxhlet extracted, roughly to quantify the residues of the target chemicals. Besides, oil phase adsorbed on the inner wall of the tube furnace were rinsed with a 30 mL mixture of acetone and *n*-hexane (1:1, v/v). Before extraction, all samples were spiked with $^{13}C_{12}$-BPA and $^{13}C_{12}$-TBBPA as internal standards. After the extracts were concentrated to 50 mL, subsamples were removed by 1, 2, and 25 mL for oil, particle, and gas samples, respectively, then dried by a gentle nitrogen stream. Finally, the samples were reconstructed in 200 μL methanol and stored at −20 °C until instrumental analysis.

2.4. Instrumental analysis

The target chemicals were quantified on a SCIEX ExionLC AD coupled with a 6500 triple quadrupole mass spectrometer (USA), with an improved method from our previous study (Ge et al., 2020). Briefly, a C18 reversed-phase analytical column (100 mm × 2.1 mm, 1.7 μm, Agilent, USA) was used. The flow rate of mobile phases (A: H_2O with 0.1 % acetic acid in volume; B: acetonitrile) was set at 0.5 mL/min, and the gradient was described as follows: 0–3 min, A: 80 %–30 %, B: 20 %–70 %; 3–10 min, A: 30 %–10 %, B: 70 %–90 %; 10–13 min, A: 10 %–10 %, B: 90 %–90 %; and 13–13.1 min, A: 10 %–80 %, B: 90 %–20 %. Other detailed instrument parameters and monitoring ions are listed in Table S1.

2.5. Quality assurance and quality controls

To ensure the polyurethane foam plug was not saturated by adsorption, another one was connected in series to calculate the penetration ratio, and the result showed that none of the target chemicals were detected. Besides, the extraction process blanks of quartz membrane and the polyurethane foam plug also showed no background interference. The extraction recoveries of the target chemicals on the quartz membrane and polyurethane foam plug were 78.1 %–105 % and 71.3 %–102 %, respectively (Table S1). The limit of detection (LOD) of each analyte was defined as 3 times that analyte's signal-to-noise ratio. The calibration curves used for quantification showed good linearity with all regression coefficients > 0.99.

2.6. Calculation of emission factor and statistical analysis

The emission factor of each analyte was calculated as follows:

$$\textit{Emission factor} = \frac{m_{\text{oil}} + m_{\text{particle}} + m_{\text{gas}}}{M},$$

where emission factor represents the mass of the chemical released by unit mass of printed circuit board (μg/g); m_{oil}, m_{particle}, and m_{gas} are the mass of the chemical in the oil, particle, and gas phase (μg), respectively; and M is the mass of printed circuit board scraps used in tube furnace experiment (g).

Analytes whose concentrations were not detected or below the LOD were reported as "n.d." or "<LOD," respectively. The significant difference between any two concentrations was tested using an independent sample *t*-test with SPSS (IBM, USA), and the significance threshold was set at $p < 0.05$. Because of the co-elution of 2-Cl-2′,6-Br_2BPA and 2-Cl-2′,6′-Br_2BPA, these two congeners were denoted 2-Cl-2′,6$^{\#}$-Br_2BPA.

2.7. Quantum chemical calculations of reaction energy

To understand better the transformation mechanisms of TBBPA, quantum chemical calculations were carried out using the Gaussian 09 program (Frisch et al., 2009). The molecular structures of the TBBPA and its transformation products were first fully optimized with DFT at the M062X/6-31G** level (Walker et al., 2013). Frequency calculations were performed to confirm the true energy minimum and to obtain the thermodynamic contributions. Considering the high-temperature combustion, all the quantum calculations were carried out in the gas phase at the combustion temperature of 300 °C under 1 atm.

3. Results and discussion

3.1. Concentrations of the target chemicals in printed circuit boards

Before investigation of the emission characteristics, the target compounds in printed circuit boards were determined. The results are shown in Table 1. This showed that TBBPA, Br_xBPAs, and BPA were found in the printed circuit boards, whereas none of the Cl_yBr_xBPAs were detected. Among them, BPA showed the highest concentration with 118 μg/g, followed by TBBPA (14.0 μg/g), 2-BrBPA (8.23 μg/g), 2,2′,6-Br_3BPA (6.16 μg/g), and 2,6-Br_2BPA (0.763 μg/g). As is well known, BPA is the main monomer for synthesizing epoxy resins, and TBBPA is added to it to increase the flame-retardant property (Bae et al., 2002; Zhou et al., 2014). Br_xBPAs may be either produced as by-products in the manufacture of commercial TBBPA (Howard and Muir, 2013), or debrominated from TBBPA residues during the production of printed circuit boards. In addition, none of the Cl_yBr_xBPAs in printed circuit boards suggested that they could not be the by-products in the manufacture of TBBPA and printed circuit boards, or added to materials as novel flame retardants. Cl_yBr_xBPAs

Table 1
Concentrations (μg/g) of the target compounds in the printed circuit board, oil phase, particle phase, and gas phase, as well as their emission factors (μg/g) in the tube furnace experiment.

Compound	Printed circuit board		Oil phase		Particle phase		Gas phase		Emission factor	
	Mean	SD [a]	Mean	SD	Mean	SD	Mean	SD	Mean	SD
TBBPA	14.0	1.87	1.00×10^3	119	248	15.7	n.d.[b]	n.d.	1.25×10^3	131
2,2′,6-Br_3BPA	6.16	1.26	2.11×10^3	193	506	37.5	n.d.	n.d.	2.61×10^3	223
2,2'-Br_2BPA	2.45	0.108	680	50.9	556	36.0	n.d.	n.d.	1.24×10^3	86.7
2,6-Br_2BPA	0.763	0.215	480	29.7	429	32.5	n.d.	n.d.	909	60.9
Σ_2Br_2BPA	3.21	0.316	1.16×10^3	79.7	985	68.1	n.d.	n.d.	2.15×10^3	148
2-BrBPA	8.23	1.46	2.30×10^3	97.2	1.68×10^3	145	6.73	2.23	3.99×10^3	244
Σ_4Br_xBPAs	17.6	2.15	5.57×10^3	364	3.18×10^3	247	6.73	2.23	8.75×10^3	605
BPA	118	23.6	1.86×10^3	118	1.32×10^3	99.6	0.257	0.169	3.18×10^3	215
2-Cl-2′,6,6′-Br_3BPA	n.d.	n.d.	72.0	11.5	11.9	1.25	n.d.	n.d.	83.9	12.5
2-Cl-2′,6$^{\#}$-Br_2BPA[c]	n.d.	n.d.	70.5	7.94	15.5	1.09	n.d.	n.d.	86.0	8.99
2-Cl-2′-BrBPA	n.d.	n.d.	40.1	4.15	35.7	2.45	n.d.	n.d.	75.8	6.56
2-Cl-6-BrBPA	n.d.	n.d.	7.96	7.23×10^{-2}	6.39	0.512	n.d.	n.d.	14.4	0.575
$\Sigma_2Cl_1Br_1$BPA	n.d.	n.d.	48.1	4.21	42.1	2.94	n.d.	n.d.	90.2	7.12
2,2′-Cl_2-6,6′-Br_2BPA	n.d.	n.d.	n.d.	n.d.	0.287	2.71×10^{-2}	n.d.	n.d.	0.287	2.71×10^{-2}
2,2'-Cl_2-6-BrBPA	n.d.	n.d.	6.14	6.22×10^{-2}	1.05	8.72×10^{-2}	n.d.	n.d.	7.19	0.620
$\Sigma_7Cl_yBr_x$BPAs	n.d.	n.d.	197	23.9	70.9	5.26	n.d.	n.d.	268	28.9

[a] Standard deviation.
[b] Not detected.
[c] Because 2-Cl-2′,6-Br_2BPA and 2-Cl-2′,6′-Br_2BPA are co-eluted, the mixture of these two compounds is denoted as 2-Cl-2′,6$^{\#}$-Br_2BPA.

can be only generated during the e-waste thermal treatment processes from precursor compounds, such as TBBPA and Br_xBPAs.

3.2. Emission factors of the target chemicals

The emission factor of each compound was determined using a tube furnace experiment under the temperature from 25 °C to 600 °C, as shown in Fig. S1. In general, Σ_4Br_xBPAs had the highest emission factor of 8.75 × 10^3 μg/g, significantly higher than 3.18 × 10^3 μg/g of BPA, 1.25 × 10^3 μg/g of TBBPA, and 268 μg/g of $\Sigma_7Cl_yBr_xBPAs$ ($p < 0.05$) (Fig. 1A, B and Table 1). The residues of TBBPA, Br_xBPA, and BPA in printed circuit boards only provided 1.1 %, 0.2 %, and 3.7 % of the corresponding emission factor, or even lower due to the transformation. Thus, all emissions could be approximated as transformed, and higher emission than the residues revealed massive amounts of fresh TBBPA and BPA were released, leading to more opportunities to produce Br_xBPAs. As expected, Cl_yBr_xBPAs were formed in the tube furnace experiment, although their emission factors were far lower than those of Br_xBPAs. Despite both being transformation products of TBBPA, a few of Br_xBPAs originated from the printed circuit board, whereas all Cl_yBr_xBPAs were formed during the combustion process. In addition, the rarer chlorine source, which may release from chlorinated flame retardants or other chlorine-containing polymers, might limit the output of Cl_yBr_xBPAs. According to the reports that analyzed elements in printed circuit boards, the content of bromine considerably exceeded chlorine (Duan et al., 2011; Grause et al., 2008).

For the debrominated products, the emission factors of Br_xBPA congeners decreased in the order 2-BrBPA (3.99 × 10^3 μg/g) > 2,2′,6-Br_3BPA (2.61 × 10^3 μg/g) > 2,2′-Br_2BPA (1.24 × 10^3 μg/g) > 2,6-Br_2BPA (909 μg/g) (Fig. 1A and Table 1). There were significant differences ($p < 0.05$) among the compounds except for 2,2′,6-Br_3BPA and Σ_2Br_2BPAs (2.61 × 10^3 μg/g vs 2.15 × 10^3 μg/g). In particular, the emission of 2,2′,6-Br_3BPA and 2-BrBPA, whose residues in the printed circuit board were lower than TBBPA and BPA, were higher than the two parent compounds. This indicated that the formation of Br_xBPAs may be bidirectional, i.e., debromination of TBBPA and bromination of BPA. For Br_2BPAs, the emission factor ratio of 2,2′-Br_2BPA to 2,6-Br_2BPA was 1.36, below the residue ratio of 3.21 in printed circuit boards. Although the two Br atoms adjacent to the "–OH" compete to form hydrogen bonds with H atoms leading to unstable molecules (Shaub, 1983), high temperature indeed decreased the ratio of 2,2′-Br_2BPA to 2,6-Br_2BPA, which should be 2 caused by unselective debromination or bromination, theoretically.

For Cl_yBr_xBPAs, the emission factors of 2-Cl-2′,6,6′-Br_3BPA (83.9 μg/g), 2-Cl-2′,$6^{\#}$-Br_2BPA (86.0 μg/g), and $\Sigma_2Cl_1Br_1BPA$ (90.2 μg/g) were relatively close, which were significantly higher than those of 2,2′-Cl_2–6-BrBPA (7.19 μg/g) and 2,2′-Cl_2–6,6′-Br_2BPA (0.287 μg/g) ($p < 0.05$) (Fig. 1B and Table 1). The results suggested that Cl_yBr_xBPA congeners containing two Cl atoms were harder to form than congeners with one Cl atom. Also, when the number of Cl atoms is the same, congeners with fewer Br atoms were more likely to be formed. Between the two Cl_1Br_1BPA congeners, a significant difference at the $p < 0.05$ level was observed. The emission factor of 2-Cl-2′-BrBPA (75.8 μg/g) was 5.26 times that for 2-Cl-6-BrBPA (14.4 μg/g), suggesting that the former chemical is easier to form than the latter, and 2-Cl-6-BrBPA has more instability, like 2,6-Br_2BPA. In general, the emission factors of transformation products indicated that the formation is not only affected by the amount of Br and Cl atoms but is also related to their positions on benzene ring.

3.3. Partitions of the target chemicals between different phases

In the present study, the partitions of the chemicals among the oil, particle, and gas phases were simply estimated by the content of the chemicals in the solvent rinse, quartz membrane, and polyurethane foam, respectively. Almost all compounds were distributed in the oil and particle

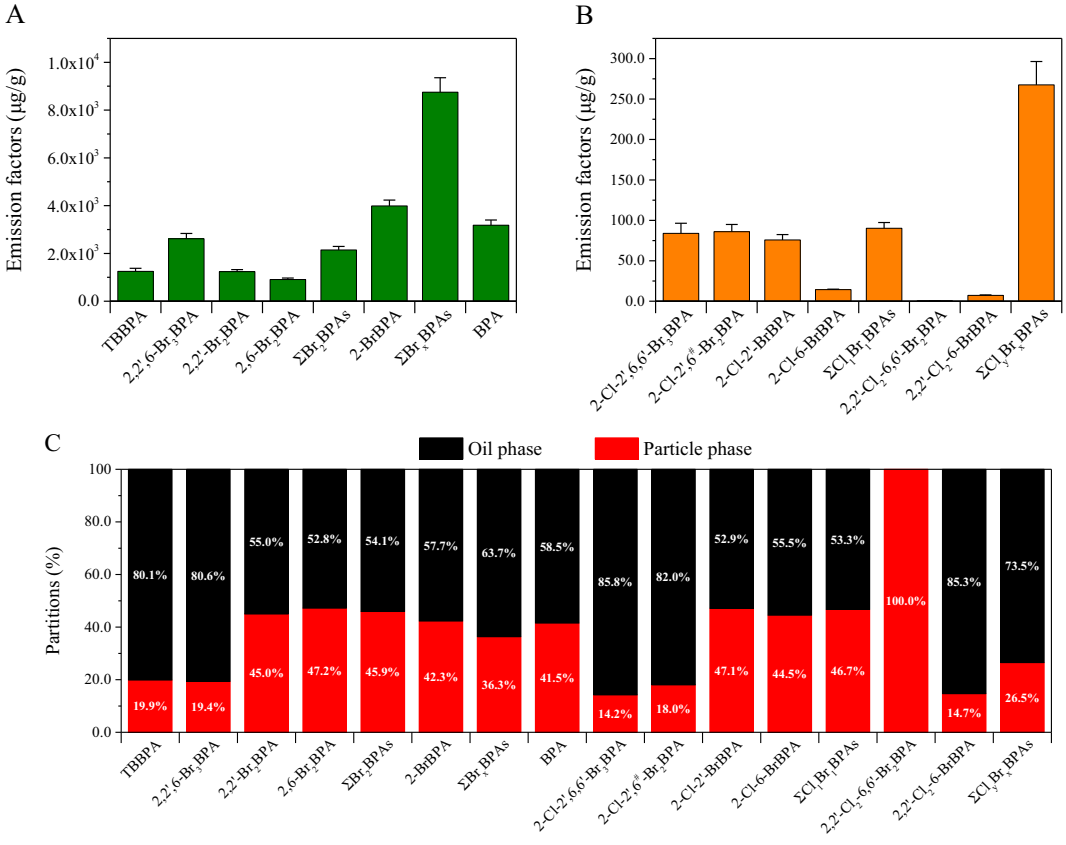

Fig. 1. Emission factors of TBBPA, Br_xBPAs, BPA (A), and Cl_yBr_xBPAs (B), and their partitions between oil and particle phases (C).

phases, with only negligible BPA at 0.257 μg/g and 2-BrBPA at 6.73 μg/g in the gas phase (Fig. 1C and Table 1). The occurrence of BPA and 2-BrBPA in the gas phase was not unexpected because their octanol–air partition coefficients (log K_{oa}) are 13.1 and 14.4, and vapor pressures are 3.68×10^{-5} Pa and 3.46×10^{-6} Pa, respectively, which are the two most volatile compounds (Table S2). The negligible gas phase chemicals may be explained by: (1) gaseous products were adsorbed by dispersed oil droplets and particles; (2) the temperature of the products in the pipeline gradually decreased, which was unfavorable for the occurrence of gaseous products; or (3) the quartz membrane that adsorbed the particle with a few of the oil droplets, like a filter cake, could further adsorb the gaseous product.

Different from the present results, studies showed that TBBPA and BPA are still partitioned in the gas phase in the atmosphere. It was reported that gaseous TBBPA ranged from 2 % to 72 % in the air in rural forest areas and seas (Xie et al., 2007), and gaseous BPA was between 28 % and 35 % in indoor and outdoor air (Moreau-Guigon et al., 2016). Therefore, we believe that direct emissions of printed circuit board combustion can also produce gaseous products, but these gaseous products will undergo the processes of adsorption and desorption by the oil and particle phases before entering the environment. In addition, compared with the passive ventilation in the present study, the suction of a pump in an active atmospheric sampler can facilitate the removal of the gas phase from the particle phase surface during sampling, and thus, lead to the different results between the present data and the literature data in air samples.

In the particle and oil phases, almost all compounds were enriched in the oil phase (52.8 %–85.8 %), with the exception of congener 2,2′-Cl_2–6,6′-Br_2BPA, which was detected 100 % in the particle phase (Fig. 1C). It was very interesting to note that those compounds containing three or four halogen atoms, including TBBPA, 2,2′,6-Br_3BPA, 2-Cl-2′,6,6′-Br_3BPA, 2-Cl-2′,6#-Br_2BPA, and 2,2′-Cl_2–6-BrBPA, were >80 % in the oil phase, which contains various complex organic compounds produced during the combustion process (Duan et al., 2012). This may be due to the high lipophilicities of the higher halogenated chemicals. Their octanol–water partition coefficients (log K_{ow}) decreased from 7.20 for TBBPA to 3.64 for BPA (Table S2). However, some particles dissolved in oil would be adsorbed on the inner wall of the tube and pipeline, and some tiny oil droplets would also be intercepted by the quartz membrane. These factors could interfere with the accurate differentiation between the two phases. In addition, the reason why 2,2′-Cl_2–6,6′-Br_2BPA is mostly in the particle phase requires further exploration. In some studies, a condensing unit was utilized to separate the oil, particle, and gas phases (Duan et al., 2011; Guo et al., 2015; Zhan et al., 2019). However, we believe that mixed tiny oil droplets and particles adsorbed gaseous products to form an aerosol, which was difficult to divide into the initial three phases by lowering the temperature. Thus, more investigations should be conducted.

3.4. Emission rates at different temperatures

Considering that the gaseous target chemicals were not detected generally and the oil products on the inner wall of the quartz tube in each temperature segment could not be obtained due to the continuous running of the tube furnace experiment and the high temperature, the emission rate curves were drawn using the compounds in the particle phase under the temperatures of 100, 200, 250, 300, 350, 400, 500, and 600 °C. As depicted in Fig. 2B, the emission rates of TBBPA, Σ_4Br_xBPAs, BPA, and $\Sigma_7Cl_yBr_x$BPAs had the same trends over temperature. From 25 to 200 °C, only BPA was detected with a concentration below the LOD, until its emission rate reached 3.67×10^{-2} μg/(g min) at 250 °C, which was also negligible (Table S3). This was evidenced by the almost constant weight of the thermogravimetric curve and the unchanged state of printed circuit board scraps (Fig. 2A and Fig. S2). When the temperature rose to 300 °C, the emission rates of TBBPA, Σ_4Br_xBPAs, BPA, and $\Sigma_7Cl_yBr_x$BPAs increased sharply, reaching 6.43, 19.7,

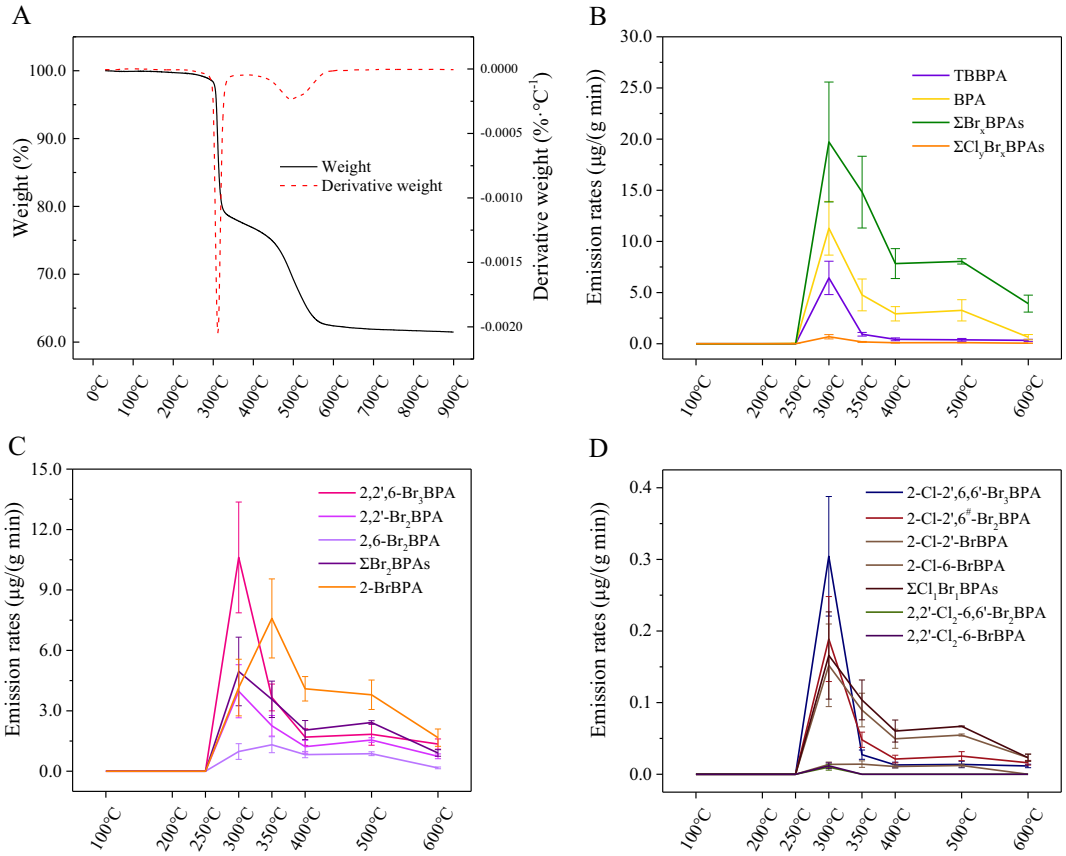

Fig. 2. Thermogravimetric curve of printed circuit board scraps (A) and emission rates of TBBPA, Br_xBPAs, BPA, and Cl_yBr_xBPAs (B), including each congener of Br_xBPAs (C) and Cl_yBr_xBPAs (D).

11.3, and 0.681 μg/(g min), respectively. Macroscopically, the printed circuit board scraps were oxidized, and an obvious weight loss occurred in the thermogravimetric curve, representing the degradation of brominated epoxy resins, releasing numerous (semi-) volatile organic compounds (Chien et al., 2000). Above 300 °C, the emission rates gradually decreased and the resins on boards turned to black char. At 500 °C, there was another weight loss in the thermogravimetric curve, indicating the further oxidation and volatilization of black char. When the temperature reached 600 °C, the resins had been combusted and only the glass-fiber cloth was left, and the target compounds would still be emitted. This may be because the oil products that were adsorbed on the inner wall of the quartz tube volatilized at a higher temperature.

As studies have reported, various additives in printed circuit boards and their transformation products were emitted in large quantities around 300 °C (Cai et al., 2018; Duan et al., 2011; Zhan et al., 2019), although printed circuit board scraps at 300 °C were not charred enough (Fig. S2). Because brominated epoxy resins often incorporate amine-containing monomers as curing agents (Levchik and Weil, 2004), a yellowed surface caused by carbonyl groups or free amines at 300 °C indicated that the long-chain polymers were broken. For example, diglycidyl ether tetrabromobisphenol/bisphenol A were common in printed circuit boards, where both 1,4H transfer and attachment of HBr on "–O–" can lead to the generation of TBBPA and BPA (Altarawneh et al., 2019; Luda et al., 2002). Moreover, in an environment rich in "•H" and "•Br," the generation of Br_xBPAs may be governed by radical substitution reactions, instead of bimolecular reactions and de novo synthesis, which mainly take place in the generation of halogenated dioxins and furans, halogenated polycyclic aromatic hydrocarbons, and other structurally altered compounds as reported in the literature (Altarawneh et al., 2009, 2019, Altarawneh and Altarawneh, 2022; Ortuno et al., 2014). As aforementioned, the amount of "•Cl" was far lower than "•H" and "•Br," leading to a low yield of Cl_yBr_xBPAs.

In detail for the individual chemicals, the highest emission rate was 10.6 μg/(g min) for 2,2′,6-Br_3BPA and 3.97 μg/(g min) for 2,2′-Br_2BPA at 300 °C, whereas 1.32 μg/(g min) for 2,6-Br_2BPA and 7.95 μg/(g min) for 2-BrBPA at 350 °C (Fig. 2C and Table S3). It was noticed that although the fastest emission temperature for 2-BrBPA was not at 300 °C, its emission rate above 350 °C was obviously higher than those of the other compounds, thus, leading to the highest emission factor. For the two Br_2BPA congeners, they could be generated in two directions as aforementioned. Specifically, 2,2′-Br_2BPA, synchronized with 2,2′,6-Br_3BPA, peaked at 300 °C, whereas 2,6-Br_2BPA, synchronized with 2-BrBPA, peaked at 350 °C. It was assumed that the process that mainly occurred at 300 °C was the debromination of 2,2′,6-Br_3BPA, and 2,2′-Br_2BPA is the main product due to the more stable molecular structure (Shaub, 1983). In addition, the main process that occurred at 350 °C was the bromination of 2-BrBPA to form 2,6-Br_2BPA, which could receive indirect evidence by the fact that the emission rate of 2,6-BrBPA was still elevated, although the emission rate increase (1.83 times) of 2-BrBPA was less than the emission rate decrease (2.90 times) of 2,2′,6-Br_3BPA from 300 to 350 °C.

For Cl_yBr_xBPAs, the highest emission rates for the congeners were observed at 300 °C except for 2-Cl-6-BrBPA, which peaked at 1.18×10^{-2} μg/(g min) at 350 °C. The emission rates for 2-Cl-2′,6,6′-Br_3BPA, 2-Cl-2′,6$^{\#}$-Br_2BPA, 2-Cl-2′-Br_2BPA, 2,2′-Cl_2–6-BrBPA, and 2,2′-Cl_2–6,6′-Br_2BPA were 0.304, 0.189, 0.152, 1.18×10^{-2}, and 9.88×10^{-3} μg/(g min) from fastest to slowest, respectively (Fig. 2D and Table S3). The trend of 2-Cl-2′,6,6′-Br_3BPA was similar to that of 2,2′,6-Br_3BPA with a peak at 300 °C, then lower than the other congeners. It was suggested that the formation of 2-Cl-2′,6,6′-Br_3BPA, as well as 2,2′,6-Br_3BPA, was from TBBPA, or 2-Cl-2′,6,6′-Br_3BPA directly transformed from 2,2′,6-Br_3BPA. Likewise, 2-Cl-2′,6$^{\#}$-Br_2BPA and the two Cl_1Br_1BPA congeners were all derived from corresponding Br_xBPAs via radical substitution reactions. Especially for 2-Cl-6-BrBPA, its emission rate curve was synchronized with that of 2-BrBPA and 2,6-Br_2BPA, further indicating that homocyclic-dihalogenated compounds were mainly formed by the halogenation process at 350 °C, although more research is needed for their transformation pathways.

3.5. Composition profiles at different temperatures

To understand clearly the emissions of the target chemicals, the composition profiles of the total emission, in which each compound was the sum in the oil, particle, and gas phases, are discussed. In addition, for the convenience of discussion, the target compounds are divided into two groups, i.e., Group A and Group B, where the former includes TBBPA, Br_xBPAs, and BPA, and the latter contains Cl_yBr_xBPAs. In the total emission, 2-BrBPA dominated at 30.3 %, followed by BPA at 24.1 % in Group A (Fig. 3A). TBBPA is also an initial additive like BPA. It accounted for 9.5 % of the total emission, which was less than that of 2,2′,6-Br_3BPA (19.8 %). For comparison, the residues of TBBPA, 2,2′,6-Br_3BPA, 2-BrBPA, and BPA accounted for 6.6 %, 4.4 %, 5.1 %, and 82.8 %, respectively. This demonstrated that high temperatures tended to debrominate TBBPA and brominate BPA rather than promote direct emission of the chemical. In Group B, 2-Cl-2′,6,6′-Br_3BPA, 2-Cl-2′,6$^{\#}$-Br_2BPA, and $\Sigma_2Cl_1Br_1$BPAs had similar proportions, constituting 31.4 %, 32.1 %, and 33.7 % of total Cl_yBr_xBPAs, respectively (Fig. 3A). Monochlorinated Br_xBPAs did not show the same pattern as their corresponding nonchlorinated precursors, implying the existing concentration of Br_xBPAs was not the main factor influencing the yield of these monochlorinated transformation products. For dichlorinated Br_xBPAs, 2,2′-Cl_2–6,6′-Br_2BPA and 2,2′-Cl_2–6-BrBPA accounted for only 0.1 % and 2.7 % of total Cl_yBr_xBPAs, respectively, which showed that the dichlorinated Br_xBPAs were more difficult to form, and 2,2′-Cl_2–6-BrBPA may have more stability than 2,2′-Cl_2–6,6′-Br_2BPA. In addition, as above described, the chemicals containing three or four halogen atoms had higher proportions in the oil phase, whereas compounds containing one or two halogen atoms including BPA had higher proportions in the particle phase. Noticeably, the composition of the oil phase was more similar to that of total emission than that of the particle phase (Fig. 3A). In addition, considering the high concentrations of target chemicals in the oil phase, the oil phase should be given a lot of attention.

To find the influence of degradation temperature on the emission compositions of the target compounds, the composition profiles of the target chemicals in the particle phase at different temperatures are shown in Fig. 3B. It was obvious that the emission compositions of Br_xBPAs and Cl_yBr_xBPAs at 300 °C were different from those at other temperatures. 2-BrBPA (11.1 %) was one-third of BPA (30.1 %) and the proportions of $\Sigma_2Cl_1Br_1$BPAs (24.4 %) were the least among the three kinds of monochlorinated Br_xBPAs. When 350 °C was reached, the emission proportion of 2-BrBPA and $\Sigma_2Cl_1Br_1$BPAs increased to 37.0 % and 50.0 %, respectively, whereas TBBPA and 2-Cl-2′,6,6′-Br_3BPA obviously decreased from 17.2 % and 44.7 % to 4.5 % and 15.2 %, respectively. This demonstrated that TBBPA debrominated to form 2,2′,6-Br_3BPA, where the removed bromine as HBr attacked long-chain polymers, releasing more BPA. In addition, we assumed that some of the bromine also existed in the form of radicals, which already have promoted the emission of 2-BrBPA at 300 °C (Czegeny et al., 2012). Meanwhile, "•Cl" led the transformation of TBBPA and 2,2′,6-Br_3BPA into 2-Cl-2′,6,6′-Br_3BPA. Considering that 2-Cl-2′,6,6′-Br_3BPA had the same trend of decreasing proportion as TBBPA, the debromination process may occur in 2-Cl-2′,6,6′-Br_3BPA as well. With the temperature increasing, the amount of "•Br" and "•Cl" increased, promoting the halogenation reaction, i.e., the formation of 2-BrBPA and two Cl_1Br_1BPA congeners. From 350 to 500 °C, the resins in the printed circuit boards were gradually combusted (Fig. S2). Without the supply of precursor compounds, i.e., TBBPA and BPA, the proportions of transformation products appeared to have reached an equilibrium. However, at 600 °C, the proportions of TBBPA, 2,2′,6-Br_3BPA, 2-Cl-2′,6,6′-Br_3BPA, and 2-Cl-2′,6$^{\#}$-Br_2BPA increased slightly, although the resins had been combusted with only glass fiber left. Whether they were formed from low-halogenated BPA at this rigid condition or other compounds were volatilized and discharged during the interval between the two samplings needs more research.

Compared with the composition patterns of the chemicals in dust, soil, and sediment from the e-waste dismantling area investigated in our previous studies (Chen et al., 2021; Ge et al., 2022; Liu et al., 2020), there were quite different patterns to the direct emission from combustion of

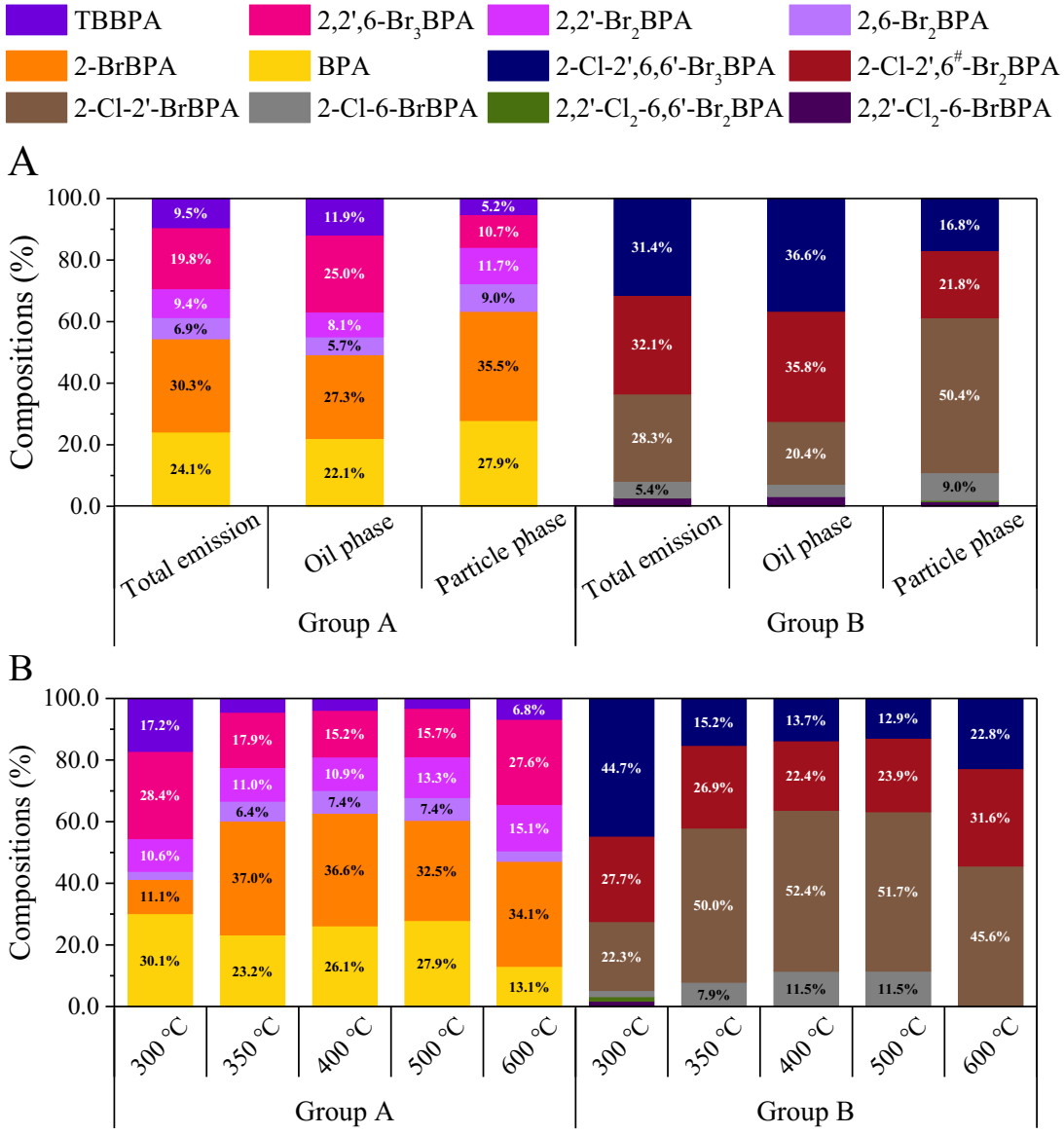

Fig. 3. Compositions of TBBPA, Br_xBPAs, BPA, and Cl_yBr_xBPAs in total emission, oil phase, and particle phase (A), and compositions of the chemicals in the particle phase at different temperatures (B). Because negligible compounds were detected, 100, 200, and 250 °C were not included. Group A includes TBBPA, Br_xBPAs, and BPA, whereas Group B only includes Cl_yBr_xBPAs.

the printed circuit boards. In the dust samples from three types of e-waste workshops (Liu et al., 2020), the compositions were similar to that of the present study, except for BPA with a negligible fraction. 2-BrBPA and monochlorinated Br_xBPAs were a large proportion of Br_xBPAs and Cl_yBr_xBPAs in the dust samples in the workshops (Liu et al., 2020). This could be attributable to the fact that the three workshops were the first station for compounds to transport into the environment. However, in the soil from the e-waste dismantling park and its surrounding area (Ge et al., 2022), the proportions of TBBPA and BPA far exceeded those of Br_xBPAs, implying that there were other sources, not only the thermal process emission. 2-Cl-2′,6,6′-Br_3BPA dominated in Cl_yBr_xBPAs, and 2,2′-Cl_2–6,6′-Br_2BPA was higher than 2,2′-Cl_2–6-BrBPA (Ge et al., 2022), which were different from the present results. In addition, in the sediment from the Lianjiang River, the dominant compound also was 2,2′-Cl_2–6,6′-Br_2BPA (Chen et al., 2021). Because the environmental matrices are complex, rich in microbes, and exposed to sunlight, degradation and transformation could occur at any time. Therefore, there may be a loss or change of source information from emissions to the environment, requiring diverse and near-to-far environmental matrices to explore the source and transport characteristics of pollutants.

3.6. Potential transformation pathways

Quantum chemical calculations were conducted separately, and the reliability of predicted transformation pathways was estimated by comparing the calculated data and experimental data. As shown in Fig. 4, the ΔG values for debromination from TBBPA to BPA were all negative (P1, P2, P3, P4, P5, and P6). This indicated that each step was spontaneous and exothermic, and BPA was the compound with the lowest energy. In contrast, the bromination from BPA to TBBPA was nonspontaneous and endothermic, where the ΔG of each step was the exact opposite of the values in the debromination process (P7, P8, P9, P10, P11, and P12). This indicated that the bromination required lots of heat, and was indirectly evidenced by the large formation of 2-BrBPA in tube furnace experiment, which represented bromination actually occurred under high temperature. Noticeably, the absolute ΔG from 2,2′,6-Br_3BPA to 2,2′-Br_2BPA (P2, $\Delta G = -28.09$ kcal/mol)

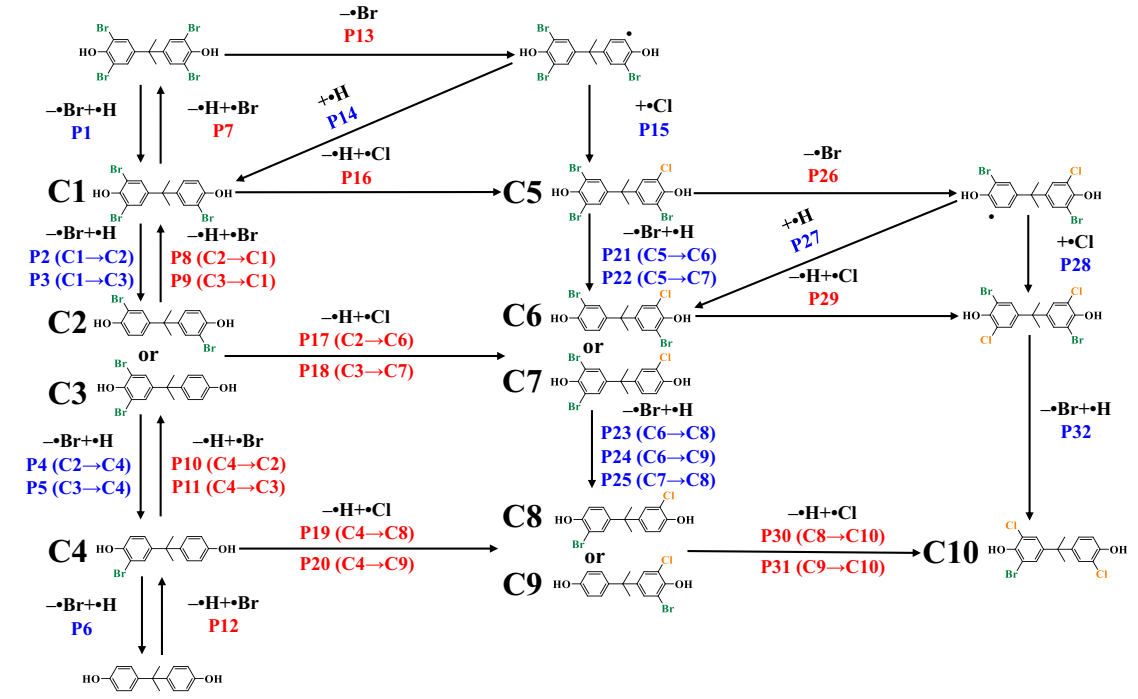

Step	ΔG	Step	ΔG	Step	ΔG	Step	ΔG
P1	–31.65	P9	27.55	P17	20.39	P25	–31.89
P2	–28.09	P10	31.10	P18	19.76	P26	91.25
P3	–27.55	P11	31.64	P19	19.51	P27	–122.23
P4	–31.10	P12	27.00	P20	23.19	P28	–99.05
P5	–31.64	P13	89.36	P21	–30.98	P29	23.18
P6	–27.00	P14	–121.01	P22	–31.07	P30	23.40
P7	31.65	P15	–97.43	P23	–31.98	P31	19.72
P8	28.09	P16	23.27	P24	–28.30	P32	–31.76

Fig. 4. The possible transformation pathways and the Δ*G* of each step (kcal/mol) calculated by quantum chemical calculation. A blue font represents a negative value of Δ*G*, whereas a red font represents a positive value of Δ*G*.

was slightly larger than that from 2,2′,6-Br_3BPA to 2,6-Br_2BPA (P3, ΔG = −27.55 kcal/mol), and the absolute ΔG from 2-BrBPA to 2,2′-Br_2BPA (P10, ΔG = 31.10 kcal/mol) was slightly smaller than that from 2-BrBPA to 2,6-Br_2BPA (P11, ΔG = 31.64 kcal/mol). This indicated that 2,2′-Br_2BPA had a more stable structure than 2,6-Br_2BPA. Although there was so little difference between the ΔG values to form two Br_2BPA congeners, 2,2′-Br_2BPA was formed >2,6-Br_2BPA in actual, which seemed to magnify the difference. Therefore, theoretical calculations could not perfectly guide what actually happened and the data should be used with caution.

In the high-temperature process, a free radical reaction is a common way of chemical transformation. For TBBPA, a single electron was exposed when "•Br" was removed (P13, ΔG = 89.36 kcal/mol), and the intermediate was extremely unstable. Once a single electron was attacked by "•H" or "•Cl," the processes are spontaneous and release heat, and a stable product would be formed. However, the ΔG through hydrogenation needed −121.01 kcal/mol (P14), whereas the ΔG through chlorination needed −97.43 kcal/mol (P15). Considering the strong electrophilicity of "•H," the hydrogen-rich environment, and the stability of the product, the probability of hydrogenation was higher, leading to the generation of Br_xBPAs in large quantities. Moreover, "•Cl" was more easily combined with "•H" than "•Br", causing chlorine would exist mainly in the form of HCl (Soderstrom and Marklund, 2022). Theoretically, the formation of Cl_yBr_xBPAs has two pathways. One is "–•H + •Cl" of Br_xBPAs, whose number of Br atoms is equal to the number of Br atoms in the corresponding Cl_yBr_xBPA product (P16, P17, P18, P19, P20, P29, P30, and P31). Another is "–•Br + •Cl" of Br_xBPAs, whose number of Br atoms is one more than the number of Br in the corresponding Cl_yBr_xBPA product (P13 + P15 and P26 + P28). The process of "–•Br + •Cl" meant the intermediate containing a single electron is combined with "•Cl" immediately. However, the former was nonspontaneous and endothermic with a positive ΔG, whereas the latter was spontaneous and exothermic with a negative ΔG. Thus, the formation of Cl_yBr_xBPAs may be mainly from "–•Br + •Cl."

For the Cl_yBr_xBPA congeners, the debromination may also take place similar to Br_xBPAs, from Cl_yBr_xBPA with three Br atoms to those with one Br atom, leading to Cl_1Br_1BPAs with a stable condition (P21, P22, P23, P24, P25, and P32). The debromination ΔG values of each step among Cl_yBr_xBPAs were close, reflected in the similar proportions of the three types of monochlorinated Br_xBPAs in the total emission. However, it was believed that the compositional difference in tube furnace experiments might be affected by molecular steric hindrance, multiple reaction pathways, and so on. Also, the bromination of Cl_1Br_1BPAs needs to be confirmed. Furthermore, the formation of dichlorinated Br_xBPAs required two consecutive spontaneous "–•Br + •Cl" (P13 + P15 + P26 + P28) or nonspontaneous "–•H + •Cl," (P17 + P29, P19 + P30, and P20 + P31) which were more difficult or had a lower conversion rate than that of monochlorinated Br_xBPAs. As a result, the emission of dichlorinated Br_xBPAs was much lower. However, it should be pointed out that the present transformation pathway proposed is only a possible pathway according to the product compositions and energy levels. In the environment, there are more factors influencing the transformation, and the transformation pathways may be more complicated.

4. Conclusions

The emission characteristics of TBBPA and its transformation products from printed circuit board scraps in combustion were systematically studied. In the tube furnace experiments under the temperature from 25 °C to 600 °C, Br_xBPAs had the highest emission factor, followed by BPA, TBBPA, and Cl_yBr_xBPAs. Among the three phases of combustion products, most compounds were found to accumulate in the oil phase more than in the particle phase. For total emission, 2-BrBPA was dominant in Br_xBPAs, and the compositions of 2-Cl-2′,6,6′-Br_3BPA, 2-Cl-2′,6$^{\#}$-Br_2BPA, and $\Sigma_2Cl_1Br_1$BPAs were approximately equal. The highest emission rates were observed at 300 °C for most target substances. The composition profiles of the chemicals at 300 °C were quite different from those at higher than 300 °C, where transformation products had larger proportions, indicating the promotion of the transformation by temperature. A radical substitution reaction was proposed mainly taking place during the transformation. According to the theoretical calculation, TBBPA, including Br_xBPAs was more prone to spontaneous and exothermic "–•Br + •H," instead of the combination of a free electron and "•Cl" when "•Br" was removed. In addition, the transformation of Cl_yBr_xBPAs from Br_xBPAs via "–•Br + •Cl" was easier than "–•H + •Cl," which was nonspontaneous and endothermic.

CRediT authorship contribution statement

Xiang Ge: Methodology, data analysis, draft writing. **Yanpeng Gao:** Methodology. **Yan Yang:** Design, methodology, data analysis, writing. **Guanhui Chen:** Methodology. **Shengtao Ma:** Methodology. **Beibei Hu:** Methodology. **Yingxin Yu:** Design, supervision, writing - review & editing. **Taicheng An:** Design.

Data availability

Data will be made available on request.

Declaration of competing interest

The authors declare that they have no known competing financial interests or personal relationships that could have appeared to influence the work reported in this paper.

Acknowledgments

The study was supported by the National Natural Science Foundation of China (41991311, 42207493, and 42277222), the Local Innovative and Research Teams Project of Guangdong Pearl River Talents Program (2017BT01Z032), Guangdong Provincial Key R&D Program (2022-GDUT-A0007), and Guangdong-Hong Kong-Macao Joint Laboratory for Contaminants Exposure and Health (2020B1212030008).

Appendix A. Supplementary data

Information related to this article can be found in Figs. S1–S2 and Tables S1–S3. Supplementary data to this article can be found online at doi:https://doi.org/10.1016/j.scitotenv.2022.160104.

References

Altarawneh, I.S., Altarawneh, M., 2022. On the formation chemistry of brominated polycyclic aromatic hydrocarbons (BrPAHs). Chemosphere 290, 133367.

Altarawneh, M., Dlugogorski, B.Z., Kennedy, E.M., Mackie, J.C., 2009. Mechanisms for formation, chlorination, dichlorination and destruction of polychlorinated dibenzo-p-dioxins and dibenzofurans (PCDD/Fs). Prog. Energy Combust. Sci. 35, 245–274.

Altarawneh, M., Saeed, A., Al-Harahsheh, M., Dlugogorski, B.Z., 2019. Thermal decomposition of brominated flame retardants (BFRs): products and mechanisms. Prog. Energy Combust. Sci. 70, 212–259.

Bae, B., Jeong, J.H., Jee, S.J., 2002. The quantification and characterization of endocrine disruptor bisphenol-A leaching from epoxy resin. Water Sci. Technol. 46, 381–387.

Barontini, F., Marsanich, K., Petarca, L., Cozzani, V., 2004. The thermal degradation process of tetrabromobisphenol A. Ind. Eng. Chem. Res. 43, 1952–1961.

Barontini, F., Marsanich, K., Petarca, L., Cozzani, V., 2005. Thermal degradation and decomposition products of electronic boards containing BFRs. Ind. Eng. Chem. Res. 44, 4186–4199.

Bendig, P., Blumenstein, M., Vetter, W., 2012. Heating of BDE-209 and BDE-47 in plant oil in presence of o, p'-DDT or iron(III) chloride can produce monochloro-polybromo diphenyl ethers. Food Chem. Toxicol. 50, 1697–1703.

Cai, C.Y., Yu, S.Y., Liu, Y., Tao, S., Liu, W.X., 2018. PBDE emission from e-wastes during the pyrolytic process: emission factor, compositional profile, size distribution, and gas-particle partitioning. Environ. Pollut. 235, 419–428.

Cai, C.Y., Chen, L.Y., Huang, H.J., Liu, Y., Yu, S.Y., Liu, Y., Tao, S., Liu, W.X., 2019. Effects of temperature on the emission of particulate matter, polycyclic aromatic hydrocarbons, and polybrominated diphenyl ethers from the thermal treatment of printed wiring boards. J. Hazard. Mater. 380, 120849.

Chen, P., Ma, S.T., Yang, Y., Qi, Z.H., Wang, Y.J., Li, G.Y., Tang, J.H., Yu, Y.X., 2021. Organophosphate flame retardants, tetrabromobisphenol A, and their transformation products in sediment of e-waste dismantling areas and the flame-retardant production base. Ecotoxicol. Environ. Saf. 225, 112717.

Chiang, H.L., Lin, K.H., 2014. Exhaust constituent emission factors of printed circuit board pyrolysis processes and its exhaust control. J. Hazard. Mater. 264, 545–551.

Chien, Y.C., Wang, H.P., Lin, K.S., Huang, Y.J., Yang, Y.W., 2000. Fate of bromine in pyrolysis of printed circuit board wastes. Chemosphere 40, 383–387.

Czegeny, Cs, Jakab, E., Blazso, M., Bhaskar, T., Sakata, Y., 2012. Thermal decomposition of polymer mixtures of PVC, PET, and ABS containing brominated flame retardant: formation of chlorinated and brominated organic compounds. J. Anal. Appl. Pyrol. 96, 69–77.

Duan, H.B., Li, J.H., Liu, Y.C., Yamazaki, N., Jiang, W., 2011. Characterization and inventory of PCDD/Fs and PBDD/Fs emissions from the incineration of waste printed circuit board. Environ. Sci. Technol. 45, 6322–6328.

Duan, H.B., Li, J.H., Liu, Y.C., Yamazaki, N., Jiang, W., 2012. Characterizing the emission of chlorinated/brominated dibenzo-p-dioxins and furans from low-temperature thermal processing of waste printed circuit board. Environ. Pollut. 161, 185–191.

Feng, A.H., Chen, S.J., Chen, M.Y., He, M.J., Luo, X.J., Mai, B.X., 2012. Hexabromocyclododecane (HBCD) and tetrabromobisphenol A (TBBPA) in riverine and estuarine sediments of the Pearl River Delta in southern China, with emphasis on spatial variability in diastereoisomer- and enantiomer-specific distribution of HBCD. Mar. Pollut. Bull. 64, 919–925.

Fernandes, A.R., Mortimer, D., Wall, R.J., Bell, D.R., Rose, M., Carr, M., Panton, S., Smith, F., 2014. Mixed halogenated dioxins/furans (PXDD/Fs) and biphenyls (PXBs) in food: occurrence and toxic equivalent exposure using specific relative potencies. Environ. Int. 73, 104–110.

Frisch, M.J., Trucks, G.W., Schlegel, H.B., Scuseria, G.E., Robb, M.A., Cheeseman, J.R., Scalmani, G., Barone, V., Mennucci, B., Petersson, G.A., Nakatsuji, H., Caricato, M., Li, X., Hratchian, H.P., Izmaylov, A.F., Bloino, J., Zheng, G., Sonnenberg, J.L., Hada, M., Ehara, M., Toyota, K., Fukuda, R., Hasegawa, J., Ishida, M., Nakajima, T., Honda, Y., Kitao, O., Nakai, H., Vreven, T., Montgomery, J.A., Peralta, J.E., Ogliaro, F., Bearpark, M., Heyd, J.J., Brothers, E., Kudin, K.N., Staroverov, V.N., Kobayashi, R., Normand, J., Raghavachari, K., Rendell, A., Burant, J.C., Iyengar, S.S., Tomasi, J., Cossi, M., Rega, N., Millam, J.M., Klene, M., Knox, J.E., Cross, J.B., Bakken, V., Adamo, C., Jaramillo, J., Gomperts, R., Stratmann, R.E., Yazyev, O., Austin, A.J., Cammi, R., Pomelli, C., Ochterski, J.W., Martin, R.L., Morokuma, K., Zakrzewski, V.G., Voth, G.A., Salvador, P., Dannenberg, J.J., Dapprich, S., Daniels, A.D., Farkas, O., Foresman, J.B., Ortiz, J.V., Cioslowski, J., Fox, D.J., 2009. Gaussian 09. Gaussian, Inc., Wallingford, CT, USA.

Ge, X., Ma, S.T., Huo, Y.P., Yang, Y., Luo, X.J., Yu, Y.X., An, T.C., 2022. Mixed bromine/chlorine transformation products of tetrabromobisphenol A: potential specific molecular markers in e-waste dismantling areas. J. Hazard. Mater. 423, 127126.

Grabda, M., Oleszek-Kudlak, S., Shibata, E., Nakamura, T., 2007. Gas phase thermodynamic properties of PBDEs, PBBs, PBPs, HBCD and TBBPA predicted using DFT method. J. Mol. Struct. THEOCHEM 822, 38–44.

Grause, G., Furusawa, M., Okuwaki, A., Yoshioka, T., 2008. Pyrolysis of tetrabromobisphenol-A containing paper laminated printed circuit boards. Chemosphere 71, 872–878.

Guo, J., Zhang, R., Xu, Z.M., 2015. PBDEs emission from waste printed wiring boards during thermal process. Environ. Sci. Technol. 49, 2716–2723.

Hall, W.J., Williams, P.T., 2007. Separation and recovery of materials from scrap printed circuit boards. Resour. Conserv. Recycl. 51, 691–709.

Howard, P.H., Muir, D.C.G., 2013. Identifying new persistent and bioaccumulative organics among chemicals in commerce. III: byproducts, impurities, and transformation products. Environ. Sci. Technol. 47, 5259–5266.

Huang, D.Y., Zhao, H.Q., Liu, C.P., Sun, C.X., 2014. Characteristics, sources, and transport of tetrabromobisphenol A and bisphenol A in soils from a typical e-waste recycling area in South China. Environ. Sci. Pollut. Res. 21, 5818–5826.

Huang, J.B., Mu, X., Luo, X.S., Meng, H.X., Wang, H., Jin, L., Li, X.S., Lai, B.S., 2021. DFT studies on pyrolysis mechanisms of tetrabromobisphenol A (TBBPA). Environ. Sci. Pollut. Res. 28, 68817–68833.

Kaya, M., 2016. Recovery of metals and nonmetals from electronic waste by physical and chemical recycling processes. Waste Manag. 57, 64–90.

Krol, P., Krol, B., Dziwinski, E., 2003. Study on the synthesis of brominated epoxy resins. J. Appl. Polym. Sci. 90, 3122–3134.

Levchik, S.V., Weil, E.D., 2004. Thermal decomposition, combustion and flame-retardancy of epoxy resins – a review of the recent literature. Polym. Int. 53, 1901–1929.

Li, T.Y., Zhou, J.F., Wu, C.C., Bao, L.J., Shi, L., Zeng, E.Y., 2018. Characteristics of polybrominated diphenyl ethers released from thermal treatment and open burning of e-waste. Environ. Sci. Technol. 52, 4650–4657.

Li, T.Y., Bao, L.J., Wu, C.C., Liu, L.Y., Wong, C.S., Zeng, E.Y., 2019a. Organophosphate flame retardants emitted from thermal treatment and open burning of e-waste. J. Hazard. Mater. 367, 390–396.

Li, T.Y., Ge, J.L., Pei, J., Bao, L.J., Wu, C.C., Zeng, E.Y., 2019b. Emissions and occupational exposure risk of halogenated flame retardants from primitive recycling of e-waste. Environ. Sci. Technol. 53, 12495–12505.

Liu, K., Li, J., Yan, S.J., Zhang, W., Li, Y., Han, D., 2016. A review of status of tetrabromobisphenol A (TBBPA) in China. Chemosphere 148, 8–20.

Liu, J., Ma, S.T., Lin, M.Q., Tang, J., Yue, C.C., Zhang, Z., Yu, Y.X., An, T.C., 2020. New mixed bromine/chlorine transformation products of tetrabromobisphenol A: synthesis and identification in dust samples from an e-waste dismantling site. Environ. Sci. Technol. 54, 12235–12244.

Luda, M.P., Balabanovich, A.I., Camino, G., 2002. Thermal decomposition of fire retardant brominated epoxy resins. J. Anal. Appl. Pyrol. 65, 25–40.

Luo, J., Hu, J.W., Wei, X.H., Fu, L.Y., Li, L.Y., 2015. Dehalogenation of persistent halogenated organic compounds: a review of computational studies and quantitative structure-property relationships. Chemosphere 131, 17–33.

Mason, Q., Zacharewski, T., Denomme, M.A., Safe, L., Safe, S., 1987. Polybrominated dibenzo-p-dioxins and related compounds: quantitative in vivo and in vitro structure-activity relationships. Toxicology 44, 245–255.

Moreau-Guigon, E., Alliot, F., Gasperi, J., Blanchard, M., Teil, M.J., Mandin, C., Chevreuil, M., 2016. Seasonal fate and gas/particle partitioning of semi-volatile organic compounds in indoor and outdoor air. Atmos. Environ. 147, 423–433.

Ni, H.G., Zeng, H., 2013. HBCD and TBBPA in particulate phase of indoor air in Shenzhen, China. Sci. Total Environ. 458, 15–19.

Ortuno, N., Conesa, J.A., Molto, J., Font, R., 2014. De novo synthesis of brominated dioxins and furans. Environ. Sci. Technol. 48, 7959–7965.

Qiu, S.S., Wei, J., Pan, F., Liu, J.P., Zhang, A.Q., 2013. Vibrational, NMR spectrum and orbital analysis of 3,3',5,5'-tetrabromobisphenol A: a combined experimental and computational study. Spectrochim. Acta Part A: Mol. Biomol. Spectrosc. 105, 38–44.

Roszko, M., Szymczyk, K., Jedrzejczak, R., 2015. Fate of PBDEs during food processing: assessment of formation of mixed chlorinated/brominated diphenyl ethers and brominated dioxins/furans. J. Environ. Sci. Health Part B 50, 884–895.

Rupp, S., Metzger, J.W., 2005. Brominated-chlorinated diphenyl ethers formed by thermolysis of polybrominated diphenyl ethers at low temperatures. Chemosphere 60, 1644–1651.

Shaub, W.M., 1983. Procedure for estimating the heats of formation of aromatic compounds. Part II. Chlorinated phenols, biphenyls, diphenyl ethers and dibenzofurans. Thermochim. Acta 62, 315–323.

Sjodin, A., Carlsson, H., Thuresson, K., Sjolin, S., Bergman, A., Ostman, C., 2001. Flame retardants in indoor air at an electronics recycling plant and at other work environments. Environ. Sci. Technol. 35, 448–454.

Soderstrom, G., Marklund, S., 2022. PBCDD and PBCDF from incineration of waste-containing brominated flame retardants. Environ. Sci. Technol. 36, 1959–1964.

Walker, M., Harvey, A.J.A., Sen, A., Dessent, C.E.H., 2013. Performance of M06, M06–2X, and M06-HF density functionals for conformationally flexible anionic clusters: M06 functionals perform better than B3LYP for a model system with dispersion and ionic hydrogen-bonding interactions. J. Phys. Chem. A 117, 12590–12600.

Wang, S., Wang, Z., Hao, C., Peijnenburg, W.J.G.M., 2019. A DFT/TDDFT study on the mechanisms of direct and indirect photodegradation of tetrabromobisphenol A in water. Chemosphere 220, 40–46.

Weber, L.W.D., Greim, H., 1997. The toxicity of brominated and mixed-halogenated dibenzo-p-dioxins and dibenzofurans: an overview. J. Toxicol. Environ. Health 50, 195–215.

Xie, Z.Y., Ebinghaus, R., Lohmann, R., Heemken, O., Caba, A., Puttmann, W., 2007. Trace determination of the flame retardant tetrabromobisphenol A in the atmosphere by gas chromatography-mass spectrometry. Anal. Chim. Acta 584, 333–342.

Xu, J., Zhang, Y., Guo, C.S., He, Y., Li, L., Meng, W., 2013. Levels and distribution of tetrabromobisphenol a and hexabromocyclododecane in Taihu Lake,China. Environ. Toxicol. Chem. 32, 2249–2255.

Yang, S.W., Wang, S.R., Wu, F.C., Yan, Z.G., Liu, H.L., 2012. Tetrabromobisphenol A: tissue distribution in fish, and seasonal variation in water and sediment of Lake Chaohu, China. Environ. Sci. Pollut. Res. 19, 4090–4096.

Zhan, F.Q., Zhang, H.J., Cao, R., Fan, Y., Xu, P.J., Chen, J.P., 2019. Release and transformation of BTBPE during the thermal treatment of flame retardant ABS plastics. Environ. Sci. Technol. 53, 185–193.

Zhou, X.Y., Guo, J., Zhang, W., Zhou, P., Deng, J.J., Lin, K.F., 2014. Tetrabromobisphenol A contamination and emission in printed circuit board production and implications for human exposure. J. Hazard. Mater. 273, 27–35.